Impact of magnetic perturbation coils on the edge radial electric field in ASDEX Upgrade

G.D.Conway, S.Fietz, H.W.Müller, M.Kočan*, T.Lunt, P.Simon, W.Suttrop, M.Maraschek, T.Happel, E.Viezzer, and ASDEX Upgrade Team

Max-Planck Institut für Plasmaphysik, Euratom-Association IPP, Garching, Germany
**ITER Organization, Route de Vinon sur Verdon, 13115 St Paul Lez Durance, France*

1. Introduction

The use of magnetic perturbation (MP) coils for modifying ELM and MHD behaviour in tokamak H-mode plasmas has attracted renewed attention in recent years. Studies have also aimed at the fundamental mechanisms behind the plasma response to the MPs. In this context, Doppler reflectometry has been used on ASDEX Upgrade (AUG) to investigate the impact of non-axisymmetric MPs on the local radial electric field E_r and turbulence behaviour in L-mode discharges. Results show a critical density n_e threshold, below which both the edge negative E_r well and near scrape-off-layer (SOL) E_r profile are strongly modified, with enhanced/reduced fluctuations. The extent of the impact depends on the MP configuration, mode parity, strength, and MP resonance condition.

2. Magnetic Perturbation (MP) coils on ASDEX Upgrade

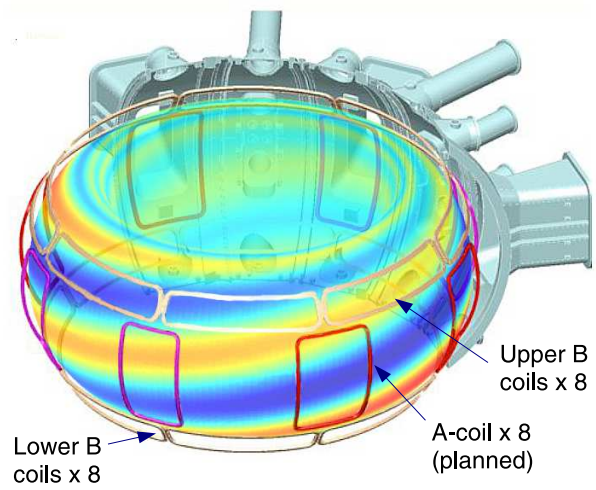

Fig. 1: *Schematic of MP coils on AUG.*

AUG currently has two sets of 8 in-vessel MP saddle coils (termed B-coils) installed on the upper and lower passive stabilizing loops, which span the full toroidal circumference, as shown in fig. 1. The coils consist of single 5-turn water cooled Cu conductors which can be connected in (anti-) series to create MPs with toroidal mode numbers of $n = 1, 2$ and 4, with variable toroidal phase Φ (orientation) in steps of 45° ($n = 1$), 90° ($n = 2$) and 180° ($n = 4$). By varying the $\Delta\Phi$ between the upper and lower coil set (i.e. parity) the alignment of the MP field with the tokamak field can be varied, and hence the degree of MP resonance with rational q surfaces. The coils are powered by two DC supplies (AC supplies currently in test) generating 5 kAt, i.e. a normalized perturbation field of $b_r/B_T \sim 10^{-3}$ [1].

3. Doppler reflectometer diagnostic

An X-mode, stepped frequency ($50 - 75$ GHz) Doppler reflectometer is used to measure the *local* $E_r \cong -2\pi f_D B_T/k_\perp$ from the Doppler frequency shift f_D in the backscattered microwave beam (for $v_{ph} \ll v_{E\times B}$ & $k_\parallel \ll k_\perp$) and the turbulence $|\delta n_e(k_\perp)|^2$ at the probed perpendicular wavenumber $k_\perp = -2N_\perp k_o$ from the integrated spectral peak $S(k_\perp)$. The

measurement location and $k_\perp$ are obtained with a beam tracing code using fitted profiles to experimental density data and *axisymmetric* equilibria [2]. The reflectometer bistatic antenna pair are located just above the lower B-coil row with an upward line of sight between B-coils 6 and 7. The diagnostic radial coverage is usually the SOL and pedestal region, but can reach to $\rho_{\rm pol} \sim 0.6$ normalized radius at very low $n_{\rm e}$.

4. Impact of MPs on edge $E_{\rm r}$

Fig. 2(a) shows the edge $E_{\rm r}$ profile for a $\bar{n}_{\rm eo} = 2 \times 10^{19}$ m^{-3}, $B_{\rm T} = -2.5$ T, $I_{\rm p} = 1.0$ MA, $q_{95} \sim 4.2$ L-mode discharge with (red) and without (blue) $n = 2$ "resonant" MPs. With a B-coil current of $I_{\rm B} = 0.9$ kA the MP impact is most pronounced. The profiles show four regions: (1) no impact on the far SOL $E_{\rm r}$, (2) a reduced near SOL $E_{\rm r}$, (3) an inversion of the $E_{\rm r}$ well, and (4) no change in $E_{\rm r}$ inside the pedestal. The $E_{\rm r}$ well inversion is not unexpected (due to ambipolarity) from an opening and/or mixing of field lines [3]. This is consistent with the computed vacuum field connection length $L_{\rm c}$ (from measurement point to divertor) shown in fig. 2(b). Without MPs $L_{\rm c}$ is small in the SOL and infinity for closed field lines (blue curve). With MPs field lines inside the separatrix begin to break and $L_{\rm c}$ drops to $1-2$ km (red curves). An MP penetration depth, ~ 1.5 cm, can be estimated from the $E_{\rm r}$ inversion radii (the outer is approximately the LCFS) - which appears narrower than the vacuum field line mixing region, implying plasma screening of the MP. Fig. 2(d) shows the corresponding $n_{\rm e}$ and $T_{\rm e}$ profiles. With MPs the energy confinement drops by $< 10\%$, but the kinetic profiles change only within error bars. For example, the edge $n_{\rm e}$ dips, but recovers by the time of the MP profile shown. The equilibrium may also experience local displacements of $\Delta r \sim 4$ mm depending on Φ [4]. However, such movements in the $n_{\rm e}$ profile or the axisymmetric equilibria used in the analysis are comparable to the intrinsic error due to the beam scattering volume. Overall, the AUG results are consistent with previous TEXTOR [3] and MAST [5] Langmuir probe measurements indicating the Doppler reflectometer measurement is robust.

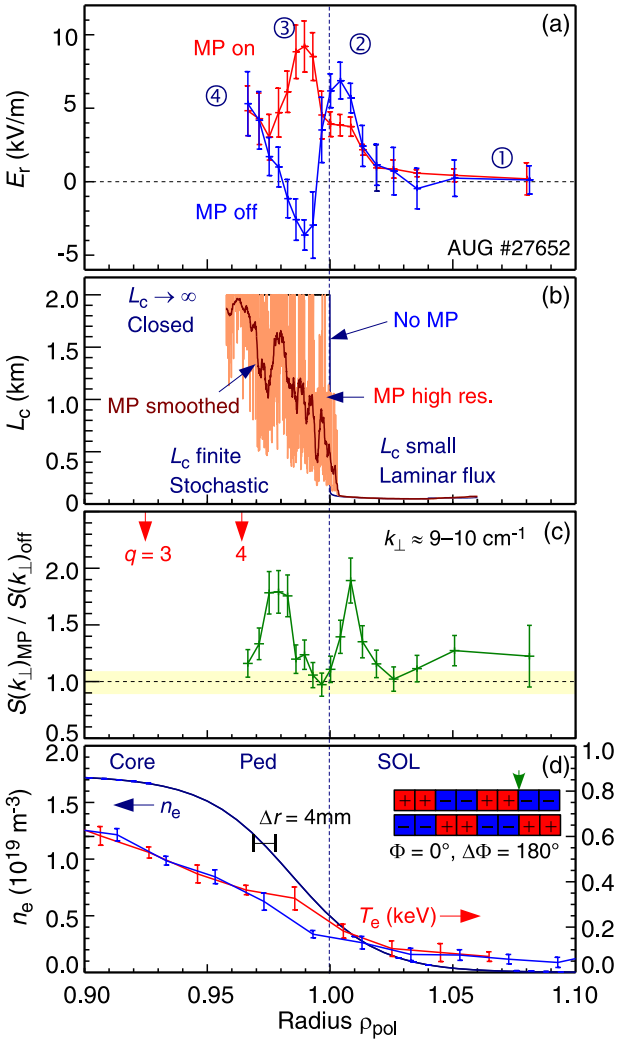

Fig. 2: (a) L-mode $E_{\rm r}$, (b) vacuum connection length $L_{\rm c}$, (c) turbulence ratio, and (d) $n_{\rm e}$ and $T_{\rm e}$ profiles with (red) and without (blue) $n = 2$, odd-parity $\Delta\Phi = 180°$, "mostly resonant" MPs.

5. MP threshold effects

A critical field $b_r/B_T \sim 10^{-4}$ is predicted [6] and observed [3,5] for MP penetration, scaling roughly linear with n_e. Fig. 3 shows such a threshold effect in the edge E_r profile during an L-mode $\bar{n}_{eo} = 2 \rightarrow 5 \times 10^{19}$ m^{-3} ramp with constant $I_B = 0.9$ kA and $n = 2$ "significantly resonant" MP configuration. As n_e (or ν^*) rises the MP impact disappears, both in the near SOL where E_r flips between reduced and non-reduced states when n_e exceeds a certain value [7]; and in the E_r well, which conversely gradually reverts to the no-MP depth with increasing n_e. This suggests distinct MP mechanisms for the laminar SOL/edge and "stochastic" pedestal regions. Similar threshold effects are observed with reversed B_T and I_p operation, as well as if the B-coil I_B is ramped with constant n_e.

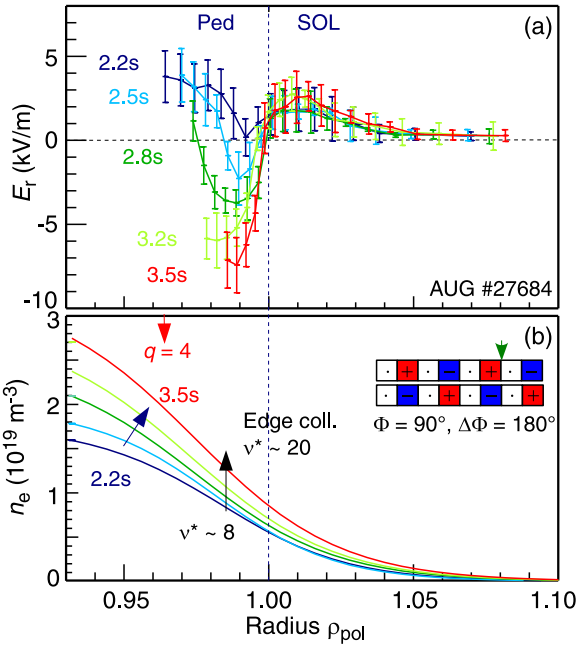

Fig. 3: (a) Edge E_r and (b) n_e profiles during an L-mode density ramp with const. $n = 2$ "resonant" MPs (-2.5 T, 1.0 MA, $q_{95} \sim 4.3$).

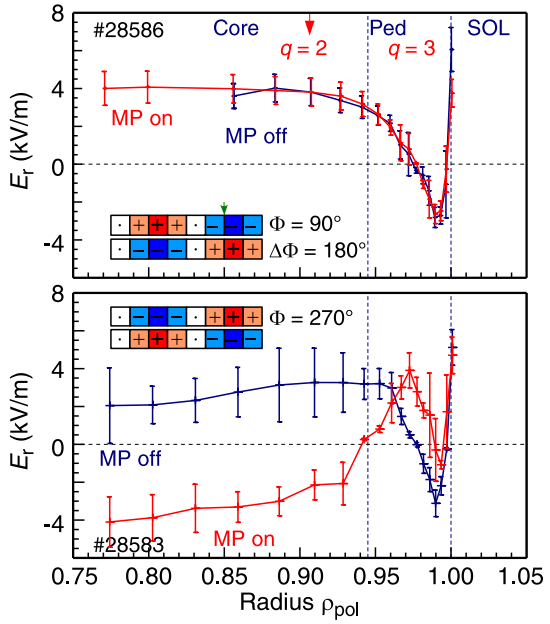

Fig. 4: L-mode E_r profiles for pairs of $n = 1$ significantly "resonant" MP toroidal phases.

6. Impact of MP toroidal phase

The MP impact varies with the B-coil toroidal phase. Fig. 4 shows a pair of L-mode E_r profiles ($I_B = 0.7$ kA, $q_{95} \sim 3$) with $n = 1$ "resonant" MPs rotated by 180°. For $\Phi = 90°$ there is no local E_r impact, while for $\Phi = 270°$ the edge E_r is up-shifted - indicating 3D MP structure. This toroidal structure is better illustrated in fig. 5 with an $n = 2$, $\Delta\Phi = 90°$ "non-resonant" configuration for $\Phi = 0, 90, 180, 270°$ MP phases. The top row shows the local E_r profiles and MP coil configuration (b_r direction) schematics. The near SOL E_r peak and the edge E_r well display individual reactions to the MP orientation - suggesting separate (but not necessarily unrelated) toroidal 3D structures for the SOL and edge regions. Fig. 4 also shows a strong core rotation reversal for $\Phi = 270°$. For this $n = 1$ phase there is significant core MHD, tending to locking (which is particularly encouraged at low n_e and q_{95} and linked to intrinsic error field interaction). The degree and radial extent of the reversal varies with the degree of mode-locking.

7. Impact of MP on turbulence level

The MP affected E_r regions are also accompanied by changes in the density turbulence level. Fig. 2(c) and bottom row of fig. 5 show the integrated spectral intensity ($S(k_\perp) \propto |\delta n_e|^2$ at the probed $k_\perp \sim 9$ cm^{-1}) with MPs normalized to the non-MP level for the respective L-mode $n = 2$ MP discharges. In the near SOL, significant changes in E_r are accompanied by a factor ~ 2 enhancement in the turbulence, while in the pedestal region δn_e may be increased (fig. 2: resonant), or decreased (fig. 5: non-resonant) depending on the MP configuration. With strongly resonant MPs the increase can be a factor of 10.

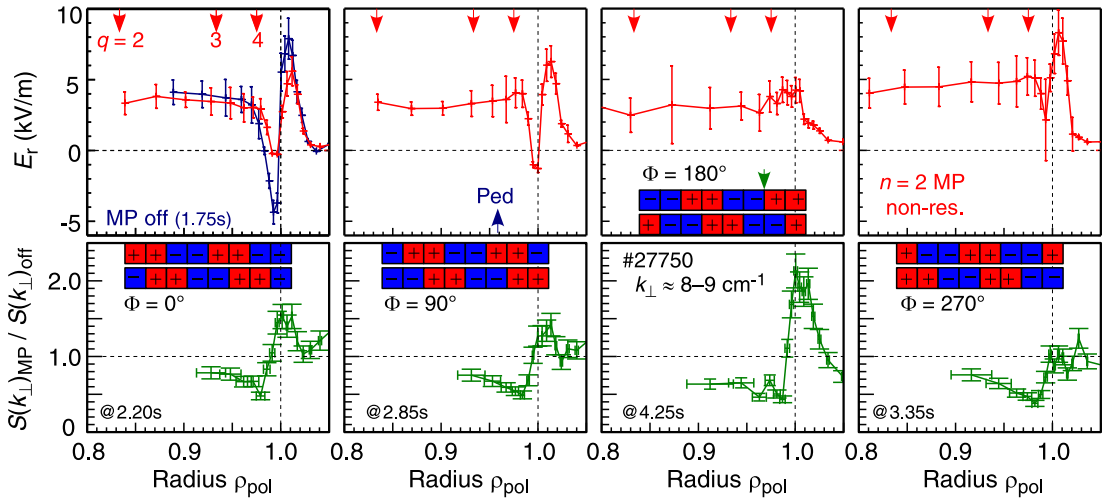

Fig. 5: (Top) E_r profiles and (bottom) turbulence enhancement factor with (red) & without (blue) $n = 2$ "non-resonant" ($\Delta\Phi = 90°$) MPs for $\Phi = 0°, 90°, 180°$ and $270°$ toroidal phases.

8. Summary & Discussion

The AUG results support previous LP measurements from other machines, specifically the reduction/reversal of the E_r well, as well as n_e and b_r thresholds linked to MP penetration. The turbulence behaviour, however, is more complicated. δn_e is generally enhanced in the near SOL, but can be enhanced or reduced across the pedestal depending on MP configuration, q profile and ∇n_e changes etc. Nevertheless, there is a clear linkage between δn_e and E_r. 3D effects are also evident. Rotating the MP coil phase reveals toroidal MP structure in both the near SOL and E_r well regions. Edge MHD (tearing modes?) in the kHz range are enhanced, coincident with the E_r well modification. Certain MP phases also promote core MHD (and mode-locking) with a consequent reduced core plasma rotation.

References

[1] W.Suttrop *et al.* Fusion Eng. Des. **84**, 290 (2009)
[2] G.D.Conway *et al.* Plasma Fusion Res. **5**, S2005 (2010)
[3] Y.Xu *et al.* Phys. Rev. Lett. **97**, 165003, (2006)
[4] J.C.Fuchs *et al.* EPS Conf. ECA **35A** P2.048 (2011)
[5] P.Tamain *et al.* Plasma Phys. Control. Fusion **52**, 075017 (2010)
[6] J.D.Callen, Nucl. Fusion **51**, 094026 (2011)
[7] H.W.Müller *et al.* J. Nucl. Mat. **438** 564 (2013)